PERIODICA POLYTECHNICA SER. CIVIL ENG. VOL. 35, NOS. 3–4, PP. 361–388 (1991)

EXAMINATIONS FOR THE DETERMINATION OF LOAD-CARRYING CAPACITY OF THE BRIDGE OVER THE SEBES-KÖRÖS AT VÉSZTŐ

GY. SZABÓ

Department of Steel Structures
Technical University, H–1521 Budapest

Received: May 31, 1992

Abstract

Load-carrying elements of a 100 years old steel (wrought iron) railway bridge have been examined. On the basis of in-situ supervision, statical analysis, in-situ and laboratory measurements conditions of the further service have been determined. The laboratory fatigue tests verified the safety of the bridge against failure.

Keywords: steel / wrought iron structure, railway bridge, reconstruction, fatigue

Introduction

The bridge over the Sebes-Körös at Vésztő is in service between sections 275 and 277 on the railway-line Dévaványa-Kótpuszta. The seven structures of deck-type, as well as the trussed river structure were constructed for the use of the local railways in county Békés in 1890.

The deck-type structures were in service supposedly in their original state for 100 years. The disadvantageous structural layout of those resulted corrosion of the parts between the overlapping surfaces of the flange-plates, which required the manufacture of new structures to replace the former ones in 1989 – 90.

The trussed bridge over the river was in service over about 70 years in its original form, then it was reinforced. The reinforced structure handled the traffic for an additional 30 year-time without any special problem to solve.

The re-building of the deck-type structures made necessary the detailed examination of the trussed structures to decide on their further functioning.

Method of Testing

To determine the load-carrying capacity of the bridge structure, tests were conducted in the following fields:

Testing of Materials

The dismounted material of the riveted plate girders over the flood-plain was at our disposal to cut out specimens, and to perform the testing of the material texture, as well as static and dynamic tests on those.

One of the stringers removed from the floor structure of the trussed bridge was subject to fatigue test.

After finishing the fatigue tests on the stringers, specimens were processed from the girder and were subject to tests similar to those performed on the material of the plate girder over the flood-plain. In this way, a possibility was provided of drawing a comparison between the two materials to determine what measure of safety can be reached in applying the statements made in the course of the detailed testing of the material of the plate girder bridge to the stringer of the trussed bridge.

Statical Analysis

Calculations were performed for the more detailed investigation of behaviour of the trussed main girder and the floor structure. In the course of calculations, the axle-load of the real vehicles (locomotives and wagons) were taken into consideration.

In-situ Measurements

With the aim of obtaining a more reliable picture of the magnitude change of the actual stresses arisen in the bridge structure, as well as with the aim of checking the results obtained in the course of calculations, electrical strain measurements were performed on the main girder and one of the stringers of the bridge.

The measurements were used for the determination of the dynamic effects depending on the speed of train passages.

The natural frequency of the bridge was determined by means of acceleration test.

Consideration Associated with Fatigue process

The overwhelming majority of the measurement procedures used in the course of design of engineering structures subject to fatigue is based on the linear cumulative damage theory. The only reason for the application of this theory consists in its unambiguous simplicity. Though its application in the course of design can be verified, however its validity is generally not backed by the experiences gained in practice and experiments.

The fatigue load-carrying capacity of the structure in question was determined from the results obtained on the basis of data known from literature, the experiments reported in literature, and our own experimental tests.

Testing of Materials

Testing of the Plate Girder Bridge over the Flood-Plain

A possibility was offered for cutting out specimens from about 1.5 m long part of the flood-plain structure destined to be demolished due to the bad corrosion damage of the flange-plates.

Owing to the fact that the flanges were corroded to a very great extent, the tests were performed, first of all, on the samples cut out of the web. The arrangement of cuts is illustrated in *Fig. 1.*

Testing of Material Texture

The texture and the slag content of the wrought iron are documented in the following photos:

Ph. No. 20	Transverse section of web	Magnification:	4.5
Ph. No. 21	Longitudinal section of web	Magnification:	4.5
Ph. No. 22	Transverse section of angle	Magnification:	4.5
Ph. No. 23	Longitudinal section of angle	Magnification:	4,5
Ph. No. 24	Longitudinal section of web	Magnification:	500
Ph. No. 25	Longitudinal section of web	Magnification:	500
Ph. No. 26	Longitudinal section of angle	Magnification:	500
Ph. No. 27	Longitudinal section of angle	Magnification:	100
Ph. No. 28	Longitudinal section of angle	Magnification:	100
Ph. No. 29	Longitudinal section of angle	Magnification:	100
Ph. No. 30	Longitudinal section of angle	Magnification:	100
Ph. No. 31	Longitudinal section of angle	Magnification:	100

Strength- and deformation properties

Within the framework of this test, the
- tensile strength
- yield point
- elongation at failure, and
- specific impact value

were determined in transverse and longitudinal directions. The tensile tests were performed on a tension-testing machine of servo-hydraulic loading system of type HUS 40.

The tensile-test diagrams were recorded by an $X-Y$ recorder. These diagrams represented the signals given by the electronic apparatus of the tension-testing machine. The method of testing fulfilled the requirements of the standard MSz 105. The specimens were of proportional, flat geometry.

Table 1

		Minimum		Average		Maximum	
		L	T	L	T	L	T
R_y	N/mm^2	234.0	240.0	238.4	241.0	240.0	241.2
R_m	N/mm^2	315.0	304.1	339.2	333.9	363.4	354.5
$\delta_{5\%}$		13	10	17.5	11.7	19	14

with the help of some special specimens. The specimen can be seen in *Fig. 3.* The tensile test was carried out with the use of a testing machine of servo hydraulic loading system of type MTS.

The registration can be seen in *Fig. 4,* while the results are shown in *Table 2.* The values recorded with the use of two types of specimen and the machine shows a satisfying agreement between the data obtained.

Table 2

		Minimum		Average		Maximum	
		L	T	L	T	L	T
R_y	N/mm^2	239.9	239.6	237.2	240.5	241.0	242.0
R_m	N/mm^2	314.9	303.9	339.7	334.0	363.1	355.1

After the completion of fatigue test, flat specimens were processed cut out from the stringer and then the most important characteristics were determined (see *Fig. 5*). The values measured on the two specimens were yielded as follows:

$$R_y = 229 \div 227\,\mathrm{N/mm^2}\,,$$
$$R_m = 324 \div 344\,\mathrm{N/mm^2}\,,$$
$$\delta_{5\%} = 17.5 \div 19.5\,.$$

The yield-point was slightly lower than the values measured on the web of the flood-plain bridge, however the other results were in fact identical.

Testing of the Specific Impact Yalue

The specimens were processed in transverse- and longitudinal directions, they were equiped with ISO V notch, and were tested at temperatures $-40°$C, $-20°$C and $+20°$C. The impact machine was a pendulu-type WPM made, and PS 30 type apparatus.

The test-results are summarized in *Table 3*.

Table 3

Temperature	Transverse			Longitudinal		
C°	1	2	3	1	2	3
−40	12	12	12	19	16	16
−20	18	18	19	22	24	29
0	20	20	18	25	24	25
+20	19	22	21	32	28	28

Fatigue Tests

From the web of the flood-plain bridge, there were processed flat specimens, specimens with flat holes, as well as specimens of circular cross-section and notches. The change in the experimental stress applied in the course of testing was a pulsating stress with $\sigma_{\min} = 0$. Testing was continued up to failure, or a cycle-number $N = 3 \cdot 10^6$. The unfailed specimens were tested again on a higher stress-level.

Nine flat-shaped specimens were subject to previous fatigue process on $\sigma = 40\,\mathrm{N/mm^2}$, then they were subject to the test mentioned above.

The results of the tests are shown if *Figs. 6, 7, 8* and *9.* In addition to the numerical results obtained, the following conclusions can be inferred from the tests:

1. There is no considerable difference between the results obtained with the specimens of longitudinal- and transverse directions.
2. The previous fatigue has no detectable effect on the cycle-number required for failure. The same can be claimed for the specimens which did not suffer failure on the first stress-level chosen under the influence of cycle- number $3 \cdot 10^6$.
3. Somewhat greater standard deviation is yielded in comparison to the steel materials used nowadays.

For the purpose of a more accurate comparison with the materials used nowadays, the results obtained with the notched specimens of a circular cross-section can serve, as shown in *Fig. 9* since the identical circumstances of the tests can be created technically with these specimens.

Fatigue-test on the Stringer of the Trussed Bridge

The stringer at the outlet side towards Vésztő of the trussed bridge was dismounted (removed). The posterior reinforcement of the joint between the stringer and cross beam was removed. Under these circumstances, the testing of the stringer took place in its original state without the posterior reinforcement. Instead of rivets removed during the disassemblage, hsfg bolts were used, they were tightened with the specified moment during assemblage, however the overlapping surfaces were left in their original state, and no surface pretreament was applied.

According to the original scheme of mounting, pieces of the sleepers, and the normal-gauge rails of type '48' were mounted on the stringer. The fatigue-load was applied by a work-cylinder positioned in the middle of the stringer. The layout can be seen in *Fig. 10.*

In the course of testing, the stresses arisen in the intermediate cross-sectional area of the stringer were measured (See *Table 4*).

The fatigue process was performed with pulsating load of $\sigma_{\min} = 0$, and cycle-number $n = 2 \cdot 10^6$ was applied for each loadstage. The load was increased by stages of 30 kN up to failure according to the following:

The failure occurred on one of the flange angles on the tension side. The crack prior to failure started from two places. In both places, the cracking started from a rivet-hole, one of them was the flame-widened place of a removed rivet, the other one was a flange-rivet in its original state. The crack propagation across the full cross- section of the flange angle occurred

Table 4

Loading	1	2	3	4
kN	σ (kN/cm^2)			
60	−3.01	−3.51	3.36	3.78
90	−4.62	−5.32	4.96	5.58
120	−5.86	−7.06	6.24	6.90
150	−7.64	−8.74	8.18	9.12
180	−9.27	−10.7	9.99	11.5

Table 5

Loading kN	Cycle-number n
90	$2 \cdot 10^6$
120	$2 \cdot 10^6$
150	$2 \cdot 10^6$
180	$1.2 \cdot 10^6$

in the cross-section of the above mentioned flange-rivet. The crack was initiated on the web, too, it was propagating in about 5 – 6 mm length above the leg of the flange in a way well observable to the naked eye. This state of the stringer was considered a failure.

In the following, by applying a load of 60 kN, the test process could be continued without any trouble. This loading-stage was continued up to cycle-number $n = 1.2 \cdot 10^6$ without any sign of the crack propagation, or any other damage to the failed girder.

Statical Analysis

Calculations were performed for the more detailed detection of the behaviour of the trussed main girder and the floor structure. In the course of our calculations, the axle-load of the real vehichles (locos, cars) were taken into account since our aim was to draw a direct comparison between the values measured and calculated in different ways. (See *Fig. 11*).

For the calculations, a computer-program (STERUE 3) developed at our Department was used. The program handles a spatial bar structure by means of the second-order theory.

On the basis of calculations, the following more important statements can be made:

- The interaction of the main girder with the floor structure (the floor structure is stressed also from the main girder effect) can be considered to be of a great extent. 25–45% of the stresses arisen in the stringer in the middle section of the bridge result from the main girder effect (depending on the load position).
- The stress-level calculated by means of the spatial model is considerably smaller than that yielded from the traditional simple model.
- The web members in both directions of the main girder take part in the load-bearing disregarding the sign of loading.

The diagrams recorded in the course of the in-situ measurement verified our calculation results.

In-situ Measurements

The in-situ measurements took place on 24 – 26 January 1991. The majority of the measuring-stations were laid out in October 1989, and this provided opportunity to perform measurements without the slightest disturbance to traffic.

Measuring Instruments

Strain-gauges were fixed at the points of the bridge as seen in *Fig. 12,* which were apt to measure the strains occurred, and to determine the magnitude of stresses subsequently.

To determine the speed of the trains passing through, at both ends of the river-bridge inductive displacement pick-ups were positioned which detected the passage of trains by measuring the deflection of the bridge.

To determine the natural bending frequency of the bridge in vertical direction, an accelerometer was positioned on the unloaded bridge.

The detailed description of the measuring, registrating and processing instruments is disregarded here.

Implementation of Measurements

The measurements were initiated with the slow passage of the loading vehicles (rail-car A 124, or 2 pieces of M32 engines) at each group of the measuring-stations — which was considered as static measurement —, then we tried to record a many passage of trains as possible at different speeds (dynamic measurements) during the period free from train-running. In the course of dynamic measurements, the scheduled Bz Mot passages were also recorded.

The natural frequency of the bridge was determined on the basis of measurements performed during periods free from trainrunning.

Realization of the Evaluation

On the basis of the diagrams recorded by a traditional recording apparatus on the site, the cases of loading (runnings) were selected which were to be evaluated with the use of a computer. The preliminary evaluation showed that the direction of the passage took no effect either on the static, or the dynamic characteristics, and further on, with respect to the dynamic characteristics it is sufficient if only a running of medium, or maximum speed (about 40 km/h) is evaluated. Accordingly, in the *Figures* with symbol VQ, the diagram of single passages at a low, medium and high speed from identical direction will be given for each measuring-station, as well as the diagram of a high-speed passage from a direction opposite to that of the former three passages is represented.

The numerical evaluation ot the diagrams can be found in *Tables 8 - 18* those contain the maximum and the minimum values of the stresses measurable in the course of the individual runnings (or one of those only if the other one is zero), as well as the read-off or calculated dynamic characteristics, respectively.

The calculation of the dynamic characteristics was performed in two ways:

a) the extreme which can be pointed out with the passage at the lowest speed as considered a static extreme was associated with the corresponding extreme of the passages at higher speeds, e. g. in this case, the dynamic factor will be:

$$\mu = \frac{\max_{\text{dyn}}}{\max_{\text{stat}}},$$

or

$$\mu = \frac{\min_{\text{dyn}}}{\min_{\text{stat}}}.$$

b) starting from the assumption that the dynamic effect results in the additional oscillation (mainly that of natural frequency) of the bridge, which will be added stochastically to the basic static effect (thus it can be added simultaneously with the reach of the extreme, too, as can be seen, e. g. in *Fig.* VQ 35), the magnitude of the maximum oscillation measurable from amplitude to amplitude downwards was read off, and the amplitude calculable from that was related to the extreme of the greater absolute value. In this case, the dynamic factor (if the value measurable from amplitude to amplitude down-ward is 2Δ) will be:

Table 7

Layout of the strain gauges for stress measurement

Layout of the measuring-station 'A'		
channel	gauge number	measured quantity
1	1	upper flange of the stringer local stress
2	2	upper flange of the stringer local stress
3	3	bottom flange of the stringer local stress
4	4	bottom flange of stringer local stress
—	—	—
6	6	acceleration
7	7	speed
Layout of the measuring station 'B'		
channel	number of gauges	measured quantity
1	$17+18+19+20$	main girder $0-1'$ aver. stress
2	$13+14+15+16$	main girder $0'-1$ aver. stress
3	$7+8$	main girder $5-4'$ aver. stress
4	$11+12$	main girder $4-5$ aver. stress
5	$5+6$	main girder $4'-5'$ aver. stress
6	$9+10$	main girder $4-5'$ aver. stress
7		speed
Layout of the measuring station 'C'		
channel	number of gauges	measured quantity
1	$17+18+19+20$	main girder $0-1'$ aver. stress
2	$13+14+15+16$	main girder $0'-1$ aver. stress
4	2	upper flange of the stringer local stress
5	3	bottom flange of the stringer local stress
6	1	upper flange of the stringer local stress
7	—	speed

Table 8
Loads (applied by the passing vehicles) recorded in the course of measurements

Serial number	Speed km/h	Layout of the measuring stations	Direction	Vehicle
1*	2.0	A	Vésztő	rail-car A 124
2		A	Szeghalom	A 124
3		A	Vésztő	A 124
4		A	Szeghalom	A 124
5*	41	A	Vésztő	A 124
6*	41		Szeghalom	A 124
7*	4.6	A	Vésztő	A 124
8		A	Szeghalom	A 124
10*	9.3	A	Szeghalom	Bz Motor train-set of 4 wagons (as scheduled)
11*	16.9	A	Vésztő	Bz motor train-set of 4 wagons (as scheduled)
12*	12.5	A	Vésztő	Bz motor rail-car as scheduled
21		B	Vésztő	Bz motor train-set as scheduled
22*	46.1	B	Szeghalom	2 × M32
23*	43.2	B	Vésztő	2 × M32
24		B	Szeghalom	2 × M32
25		B	Vésztő	2 × M32
26*	28.1	B	Szeghalom	2 × M32
27			Vésztő	2 × M32
28*	11.8	B	Szeghalom	2 × M32
29		B	Szeghalom	Bz motor train-set as scheduled
31		C	Vésztő	2 × M32
32		C	Szeghalom	2 × M32
33*	38.0	C	Vésztő	2 × M32
34*	44.0	C	Szeghalom	2 × M32
35		C	Vésztő	2 × M32
36		C	Szeghalom	2 × M32
37		C	Vésztő	2 × M32
38*	23.4	C	Szeghalom	2 × M32
39		C	Vésztő	2 × M32
40*	10.9	C	Szeghalom	2 × M32

* In the case of loads indicated by * (asterisk), the time-functions of the registrated stresses are reported.

Table 9

Number of gauge:1				Type of load: $2 \times$ M32 (VQ.46)		
	Stresses MPa			Dynamic factor		
	maximum	minimum	delta	max/statmax	min/statmin	delta/absmax
Stat	8.4	7.6	—	—	—	—
Din1	8.4	8.1	1.2	1.0	1.07	1.07
Din2	8.4	7.4	0.5	1.0	—	1.03
Din3	7	6.5	0.5	—	—	1.03

Number gauge 1				Type of load: A 124 (VQ.11)		
	Stresses MPa			Dynamic factor		
	maximum	minimum	delta	max/statmax	min/statmin	delta/absmax
Stat	4.6	-6.4	—	—	—	—
Din1	4.6	-6.6	—	(1.00)	1.03	—
Din2	5.5	-6.9	0.6	(1.20)	1.08	1.05
Din3	5.3	-7.2	0.9	(1.15)	1.13	1.07

$$\mu = 1 + \frac{\Delta}{\max_{stat}}$$

or

$$\mu = 1 + \frac{\Delta}{\min_{stat}} .$$

In the diagrams mentioned above, the values lying in the basis of calculation were indicated.

The natural frequency of the bridge was given as the average power-spectrum of the 21 series of measurements.

Considerations Associated with Fatigue Process

The loads and effects applied to the bridge during its service-life of about 100 years can be determined only by an approximation of wide outline. However, the reliable determination of the measure of fatigue damage runs into further difficulties. As an illustration of this, the article listed in the

Table 10

Number gauge 2				Type of load 2 × M32 (VQ.44)		
	Stresses MPa			Dynamic factor		
	maximum	minimum	delta	max/statmax	min/statmin	delta/absmax
Stat	11	-14.5	—	—	—	—
Din1	12.1	-16.1	1.0	1.10	1.11	1.04
Din2	9.2	-16.2	0.7	—	1.12	1.02
Din3	11	-16.8	0.1	1	1.16	1

Number of gauge: 3				Type of load: A 124		
	Stresses MPa			Dynamic load		
	maximum	minimum	delta	max/statmax	min/statmin	delta/absmax
Stat	6.1	-20.1	—	—	—	—
Din1	7	-20.0	1.0	(1.14)	—	1.02
Din2	6.5	-15	0.8	(1.06)	—	1.02
Din3	7	-19	0.9	(1.14)	—	1.02

Appendix based on literature data can serve. In this way, the calculation method based on the loads and effect, and using a suitable cumulative damage theory does not seem to look as a very promising method.

In the following, the factual pieces of knowledge will be treated one by one which are available on the basis of the tests performed hitherto. These are the following:

1. No fatigue damage or the sign of it was found on the bridge structure during the service-life of about 100 years after a thorough examination.
2. No fatigue damage was brought about to the structure by effect of the traffic flow started from 1 December 1989, or no sign of it could be detected on the structure up to the time-point of our in-situ measurements, i. e. up to 25 January 1990.
3. It can be determined on the basis of the laboratory tests carried out on the stringer removed from the floor structure of the bridge that the stringer could carry the following loads without any damage to it:

   90 kN with cycle-number 2.10^6

   120 kN with cycle-number 2.10^6

   150 kN with cycle-number 2.10^6

Table 11

Number of gauge: 3				Type of load 2 × M32 (VQ.45)		
	Stresses	MPa			Dynamic load	
	maximum	minimum	delta	max/statmax	min/statmin	delta/absmax
Stat	22	−2	—	—	—	—
Din1	23.5	−2.2	1.8	1.07	—	1.04
Din2	22.1	−2	0.9	1.01	—	1.02
Din3	26.5	−1.8	1.2	1.20	—	1.03

Number of gauge 3				Type of load A 124 (VQ.13)		
	Stresses	MPa			Dynamic load	
	maximum	minimum	delta	max/statmax	min/statmin	delta/absmax
Stat	18.1	−0.9	—	—	—	—
Din1	18.6	−1.8	0.5	1.03	—	1.01
Din2	18.1	−1.8	1.3	—	—	1.04
Din3	19.8	−2.2	1.4	1.09	—	1.04

Table 12

Number gauge 4				Type of load: A 124 (VQ.14)		
	Stresses	MPa			Dynamic factor	
	maximum	minimum	delta	max/statmax	min/statmin	delta/absmax
Stat	18.6	−1.1	—	—	—	—
Din1	19.2	−1.5	0.9	1.03	—	1.01
Din2	18	−1.9	0.9	—	—	1.02
Din3	19.3	−1.9	1.7	1.04	—	1.04

In the case of a load of 180 kN, the failure occurred after a cycle-number $n = 1.200.000$ on one of the bottom flange angle in tension.

With all this done, the failed stringer could bear a load of 60 kN without any serious damage to it up to cycle-number $n = 1.2 \cdot 10^6$ till the end of testing.

Table 13

Number gauge 13 + 14 + 15 + 16 Type of load: 2 × M32 (VQ.42)

	Stresses	MPa		Dynamic factor		
	maximum	minimum	delta	max/statmax	min/statmin	delta/absmax
Stat	0	-24.8	—	—	—	—
Din1	0	-26.0	0.9	—	1.05	1.02
Din2	—	-26.2	1.2	—	1.06	1.02
Din3	—	-26.3	1.1	—	1.06	1.02

Number gauge 13 + 14 + 15 + 16 Type of load: 2 × M32 (VQ.32)

	Stresses	MPa		Dynamic factor		
	maximum	minimum	delta	max/statmax	min/statmin	delta/absmax
Stat	—	-26.5	—	—	—	—
Din1	—	-28.8	1.4	—	1.09	1.03
Din2	—	-26.9	1.6	—	1.02	1.03
Din3	—	-26.4	1.5	—	—	1.03

From those said above, it follows that in the case of the development of a crack, there is still enough time available for the recognition of the failure and for making the necessary arrangements to repair it.

4. According to the laboratory tests performed on the specimens, it was stated that the wrought iron material of the bridge structure has a strength smaller by about 12-20 than the steel used today with respect to fatigue (37C, MSZ 6280 – 82, see *Fig. 9*).
5. From the laboratory tests performed on the specimens, it can be determined that by the effect of a previous fatigue $= 4\,\mathrm{kN/cm^2}$, the fatigue strength of the wrought iron was not reduced.

On the basis of the comparison between the test result and the in-situ measurements, as well as those of computer-aided calculations, it can be rendered probable that the overwhelming majority of the vehicles passing through the bridge during its service-life of about 100 years could not cause any considerable fatigue damage to the bridge structure.

(At the same time, it should be noted that the incompetent interventions can involve very serious danger to the structure.) The first crack, during the fatigue process of the stringer started from a flame-widened rivet-hole.)

Table 14

Number gauge 17 + 18 + 19 + 20			Type of load: 2 × M32 (VQ.41)			
	Stresses MPa			Dynamic factor		
	maximum	minimum	delta	max/statmax	min/statmin	delta/absmax
Stat	26.8	—	—	—	—	—
Din1	27	—	1.2	1.01	—	1.02
Din2	28	—	1.0	1.04	—	1.02
Din3	28.5	—	0.9	1.06	—	1.02

Number gauge 17 + 18 + 19 + 20			Type of load: 2 × M32 (VQ.31)			
	Stresses MPa			Dynamic factor		
	maximum	minimum	delta	max/statmax	min/statmin	delta/absmax
Stat	26.1	—	—	—	—	—
Din1	26.2	—	1.0	—	—	1.02
Din2	26.7	—	1.6	1.06	—	1.03
Din3	26.9	—	3.0	1.03	—	1.06

Table 15

Number gauge 9 – 10			Type of load: 2 × M32 (VQ.36)			
	Stresses MPa			Dynamic factor		
	maximum	minimum	delta	max/statmax	min/statmin	delta/absmax
Stat	34	-14	—	—	—	—
Din1	34	-13.8	2.3	1	—	1.03
Din2	34	-13.8	1.2	1	—	1.02
Din3	35	-14.2	1.2	1.03	1.01	1.02

From the above said, it can be rendered probable that the conditions for a long-range further service-life if the bridge structure can be created with respect to fatigue, too.

Table 16

Number gauge 5 – 6				Type of load: 2 × M32 (VQ.35)		
	Stresses	MPa		Dynamic factor		
	maximum	minimum	delta	max/statmax	min/statmin	delta/absmax
Stat	20.5	—	—	—	—	—
Din1	21	—	2.5	1.02	—	1.06
Din2	21.2	—	2.8	1.03	—	1.07
Din3	20.8	—	3.1	1.01	—	1.07

Table 17

Number gauge 11 – 12				Type of load: 2 × M32 (VQ.34)		
	Stresses	MPa		Dynamic factor		
	maximum	minimum	delta	max/statmax	min/statmin	delta/absmax
Stat	—	–31.5	—	—	—	—
Din1	—	–32.6	2.8	—	1.03	1.04
Din2	—	–32.4	2.9	—	1.03	1.05
Din3	—	–32.4	3.8	—	1.02	1.06

Table 18

Number gauge 7 – 8				Type of load: 2 × M32 (VQ.33)		
	Stresses	MPa		Dynamic factor		
	maximum	minimum	delta	max/statmax	min/statmin	delta/absmax
Stat	14	–31.8	—	—	—	—
Din1	14	–32.1	—	1.0	1.01	—
Din2	13.8	–32.1	0.8	—	1.01	1.01
Din3	14	–32	0.7	1.0	1.01	1.01

Further Maintenance of the Bridge

On the basis of our tests performed, the further long-range serviceability of the bridge is considered a real possibility with a satisfactory safety.

The good technical state of the bridge should be maintained continuously.

With the satisfactory technical condition preserved, all the vehicle can pass through the trussed bridge at a max. speed of 40 km/h whose axle-load does not exceed 12 tons, i. e:

- Bz rail-vons and trailers
- locomotives M28
- locomotives M32
- locomotives M43-47
- two-axle railway-wagons
- four-axle railway-wagons
- six-axle railway-wagons

The prescription of vehicle-runnings at a speed of max.40 km/h through the bridge is verified by the very low value of the dynamic factor obtained by processing the in-situ measurement data. The determined dynamic factor ($\mu = 1.2$) is the maximum value occurred in the course of measurements, and as it can be inferred from the description of the evaluation, it is not simultaneous with the maximum stress.

A later reduction in speed can be verified by the change occuring meanwhile in the technical state of the bridge.

The permission of the 12 t axle-load is backed — with respect to fatigue-load — by the adequate safety based on the test performed and the experiences gained in practice:

- On the basis of the laboratory fatigue-test performed on the stringer, with an axler-load of 12 t taken as a basis, a safety factor:

$$\nu = \frac{15}{6} = 2.5$$

is yielded against the occurrence of fatigue failure.

- Even after the possible development of the fatigue-failure on the floor system observable to the naked eye, there is still enough time available for making the necessary arrangements. Therefore, the supervision of the bridge at every 6 months is considered indispensable.
- On the basis of in-situ measurements, as well the computer-aided calculations, it can be stated that the actual behaviour and the exploitation of the bridge structure is more favourable than that yielded from the calculations performed on a traditional way.

From the load arrangements PÁLYA 13 INP and PÁLYA 15 INP of the computer-calculation, the following were yielded with respect to the stresses in bars 5 – 8 (6 – 9):
in the upper flange (point No. 8)

$$\sigma_{\max} = 1.09\,\mathrm{kN/cm^2}$$
$$\sigma_{\min} = -3.82\,\mathrm{kN/cm^2}$$
$$\sigma_{\max} - \sigma_{\min} = 4.91\,\mathrm{kN/cm^2}$$

in the bottom flange (point No. 4):

$$\sigma_{\max} = -3.79\,\mathrm{kN/cm^2}$$
$$\sigma_{\min} = -1.00\,\mathrm{kN/cm^2}$$
$$\sigma_{\max} - \sigma_{\min} = 4.79\,\mathrm{kN/cm^2}$$

When changing over to the bored cross-sectional area (1.16), as well as from the average chord stress to the extreme fibre stress (1.1), and with the dynamic factor $\mu = 1.2$ taken as a basis, $\Delta\sigma = 7.52\,\mathrm{kN/cm^2}$ will be yielded to be taken into consideration with respect to fatigue.

On identical principles, with the above values determined also for further load arrangements, the quantities contained in the *Table* are obtained.

Table 19

Load	Stringer $\Delta\sigma\,(\mathrm{kN/cm^2})$	Vehicle
13 – 15 INP	7.52	M41
14 – 16 INP	5.82	3T
17 – 19 INP	5.0	M32

With respect to the stress measured during the fatigue process of the stringer not causing failure yet, $\sigma = 9.12\,\mathrm{kN/cm^2}$ (see *Table 4*), the measure of safety against the development of a crack with an M41 vehicle will be:

$$\nu = \frac{9.12}{7.52} = 1.21$$

while with the subsequent vehicles causing smaller stresses

$$\nu = \frac{9.12}{5.82} = 1.57(\text{3 T wagon})$$
$$\nu = \frac{9.12}{5.0} = 1.82(\text{M32 loco})$$

Photo 1

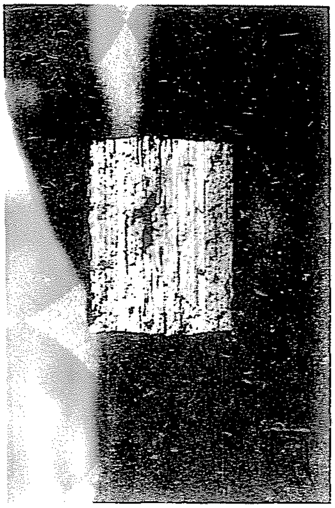

Photo 2

Photo 3

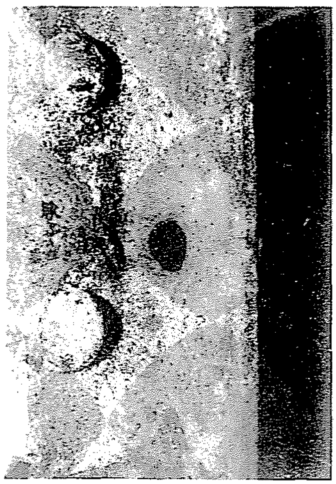

Photo 4

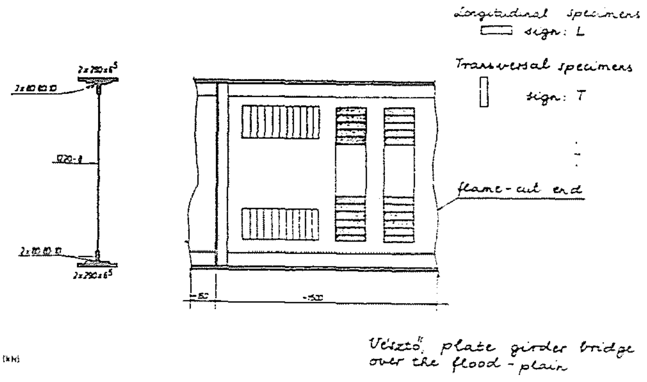

Fig. 1.

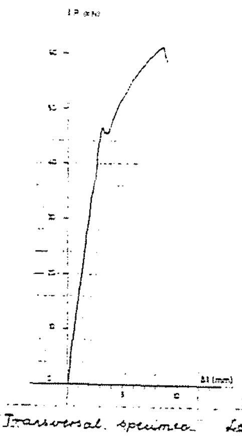

Fig. 2a.

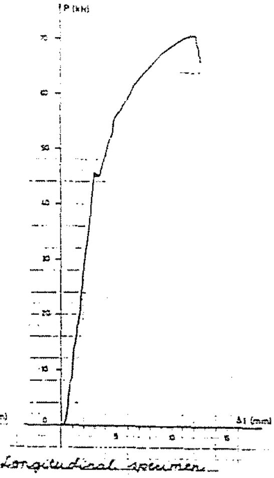

Fig. 2b.

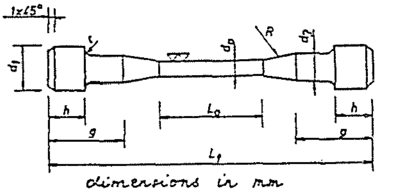

L	d_1	h	g	d_2	d_0	L_0	r	R
100	14	11	23	9	6,4	32	1	35

Fig. 3.

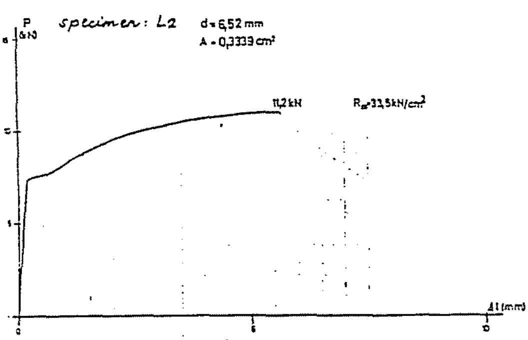

Fig. 4a.

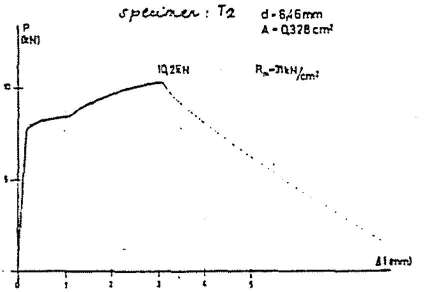

Fig. 4b.

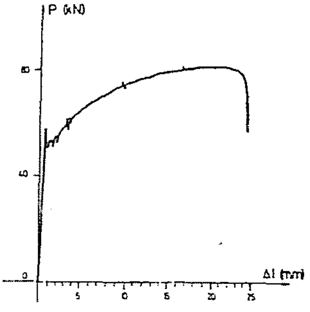

Fig. 5a.

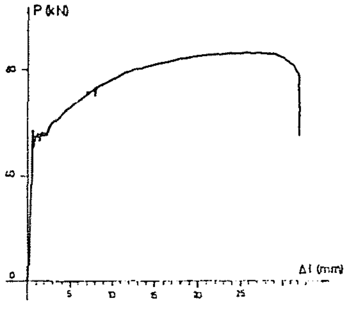

Fig. 5b.

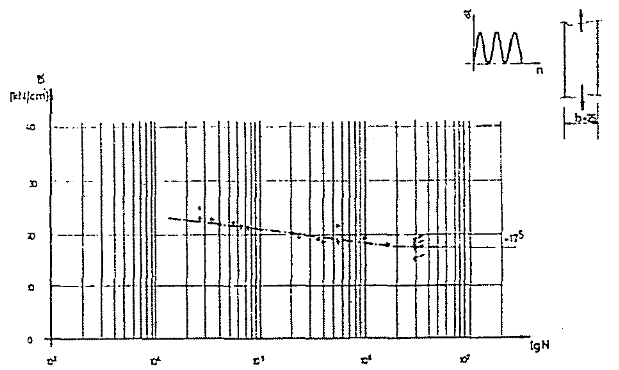

Fig. 6. Fatigue results of flat specimens

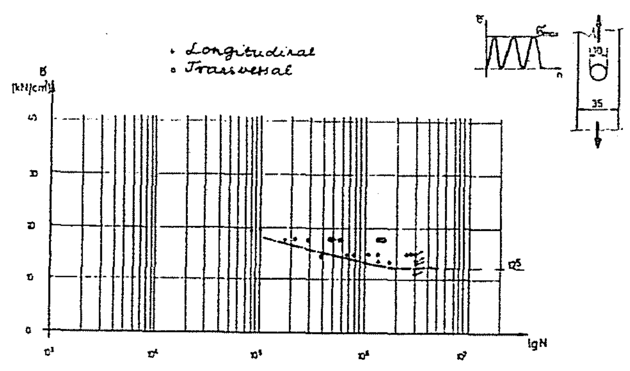

Fig. 7. Fatigue results of bored specimens

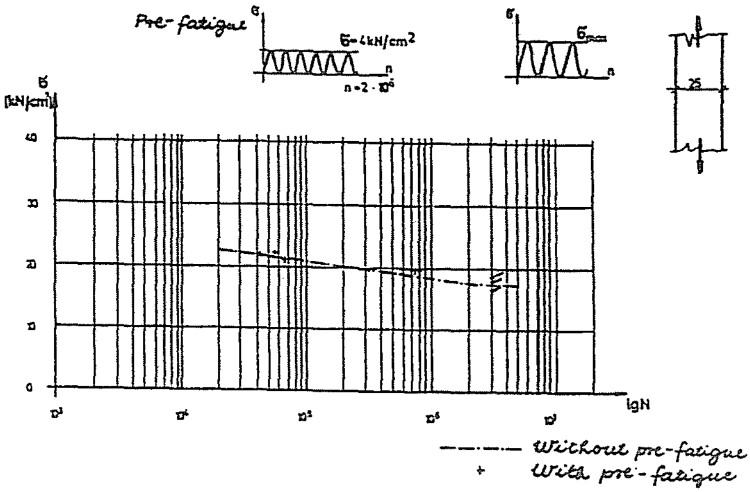

Fig. 8. Fatigue results of specimens subject to previous fatigue

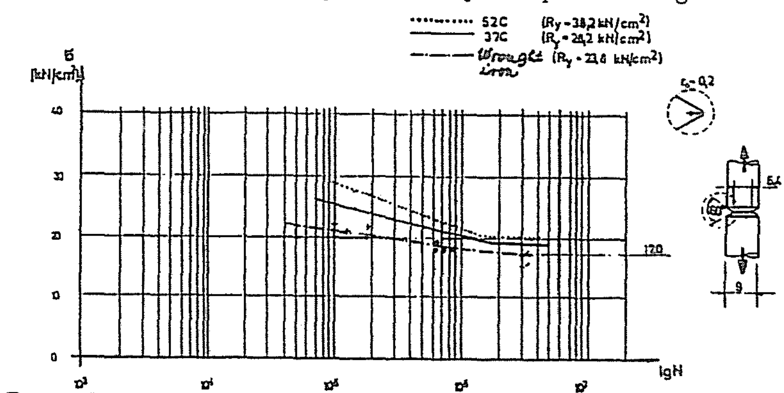

Fig. 9. Fatigue results of notched specimens with circular cross section

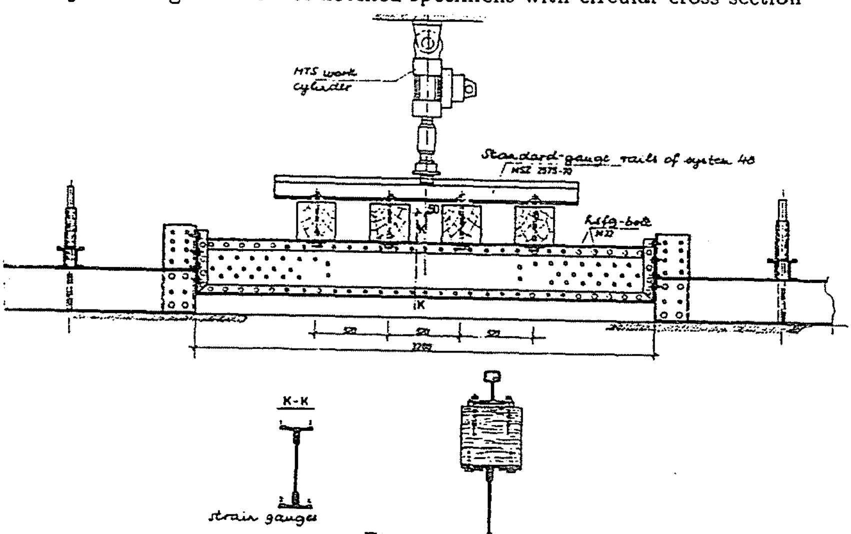

Fig. 10.

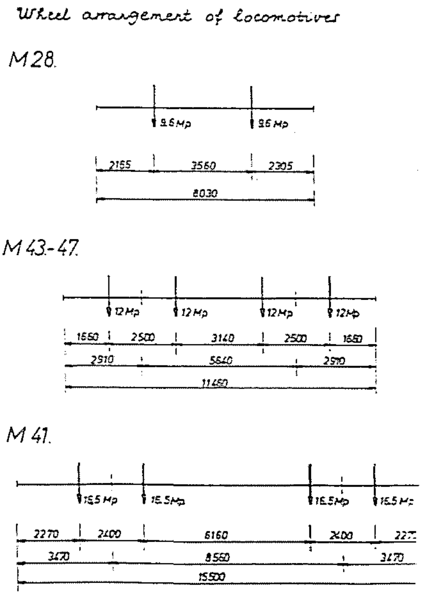

Fig. 11a.

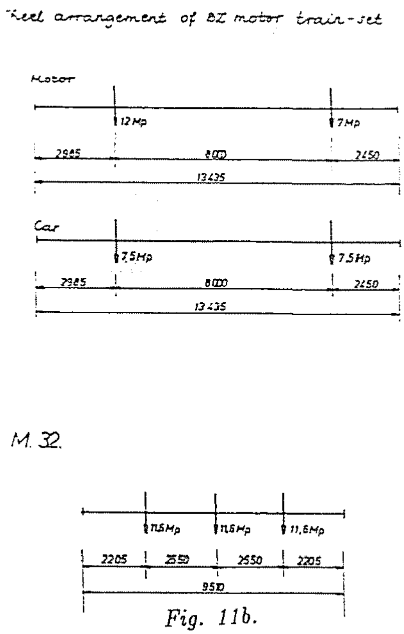

Fig. 11b.

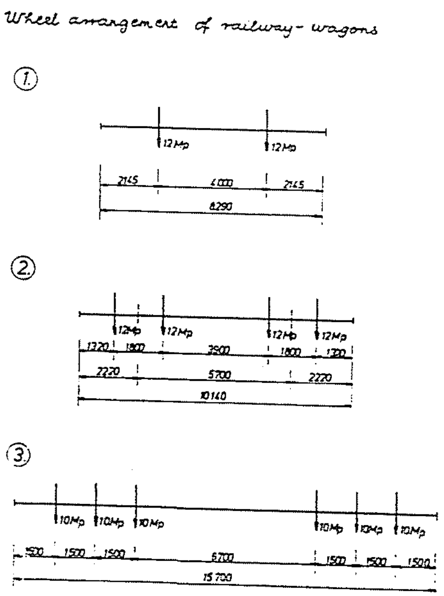

Fig. 11c.

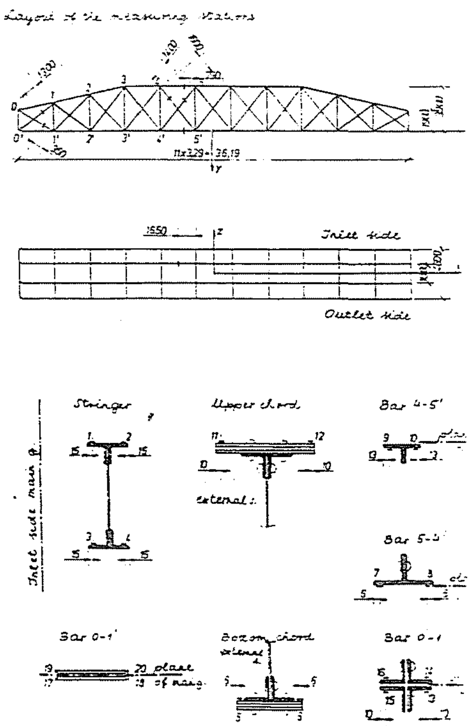

Fig. 12.

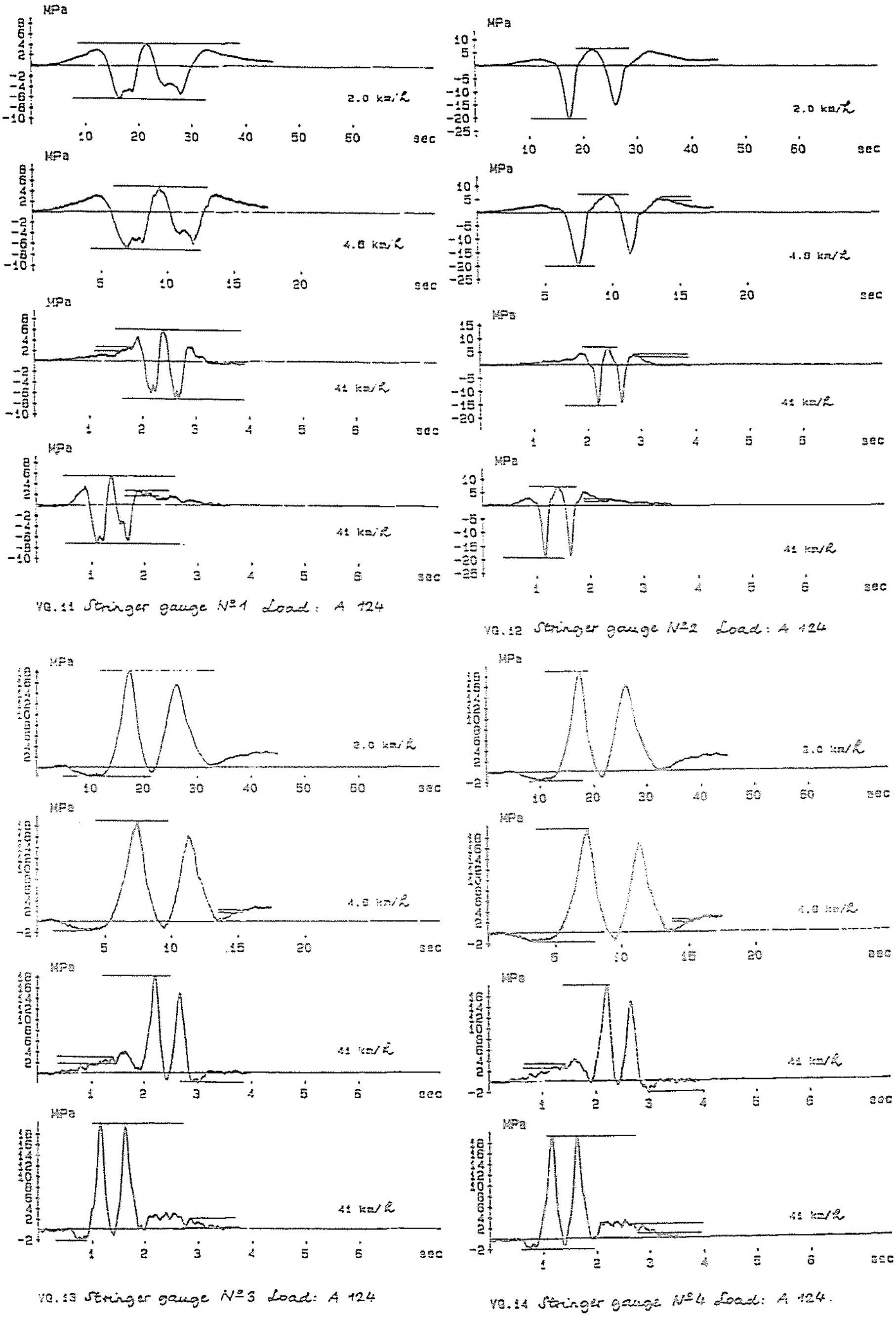
MPa
2.0 km/h
4.8 km/h
41 km/h
sec
VG.11 Stringer gauge N°1 Load: A 124
VG.12 Stringer gauge N°2 Load: A 124
VG.13 Stringer gauge N°3 Load: A 124
VG.14 Stringer gauge N°4 Load: A 124.

Fig. 13.

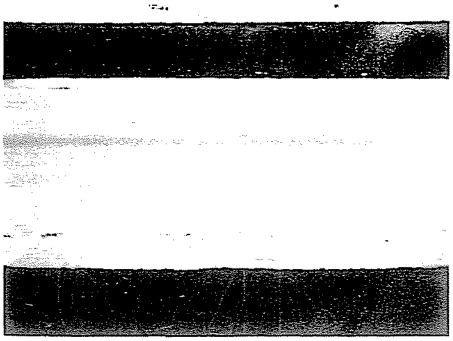

Photo 5

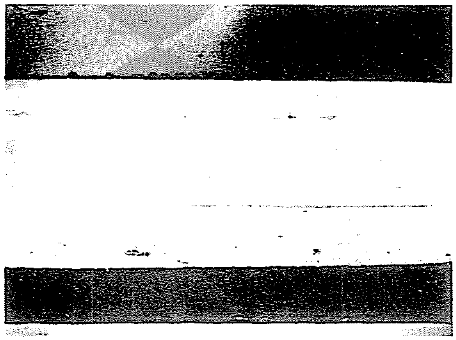

Photo 6

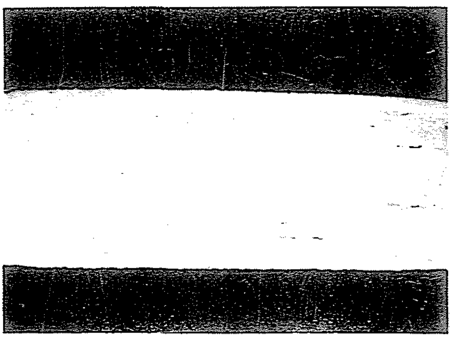

Photo 7

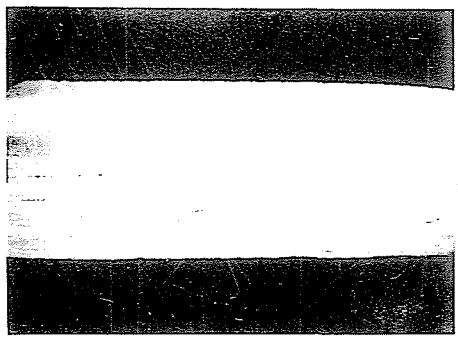

Photo 8

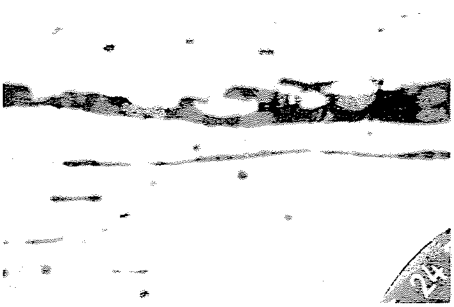

Photo 9

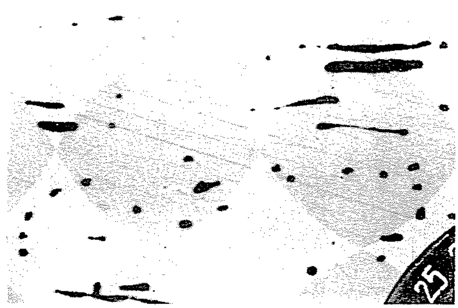

Photo 10

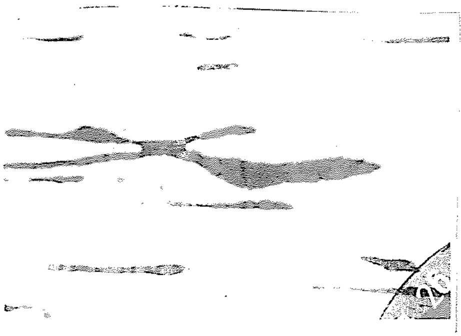

Photo 11

Photo 12

Photo 12

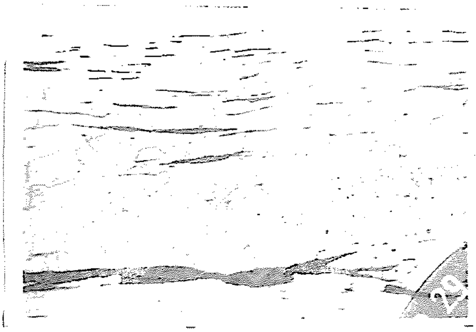

Photo 14

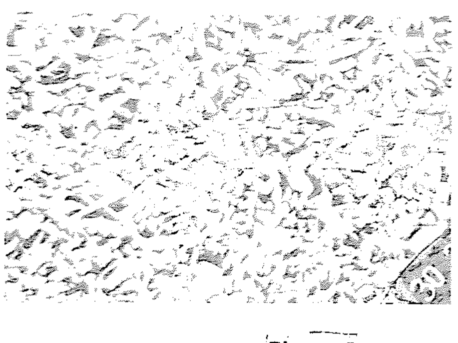

Photo 15

Photo 16

On the basis of the above formulae, with the case $\nu \geq 1.5$ considered to be of satisfactory safety, the running of all the vehicles in question — with the expection of vehicle M41 — can be permitted.

The state of the main girders is more favourable than that of the floor structure. With the fact taken into consideration that no flamewidened hole could be found on the main girder, thus when investigating the development of fatigue cracks we start from the fatigue-strength obtained with the bored specimen. ($\sigma = 12.5\,\mathrm{kN/cm^2}$).

With values mentioned earlier: $\nu = 1.5$ and $\nu = 1.2$ taken into consideration, the main girder can be considered of a satisfactory safety until formula:

$$\Delta\sigma \leq \frac{12.5}{1.5} \cdot 1.2 = 6.94\,\mathrm{kN/cm^2}$$

holds.

This condition will be fulfilled for each case tested. (The main girder was not tested with the use of M41 locomotive).

Address:

Gy. SZABÓ
Department of Steel Structures
Technical University, H–1521 Budapest